



PERFORMANCE TESTING OF A PARABOLIC TROUGH COLLECTOR ARRAY FOR A SMALL-SCALE PROCESS HEAT APPLICATION

İbrahim Halil YILMAZ*, Hakan HAYTA**, Recep YUMRUTAŞ** and Mehmet Sait SÖYLEMEZ**

*Department of Automotive Engineering, Adana Science and Technology University, Adana, Turkey
iyilmaz@adanabtu.edu.tr

**Department of Mechanical Engineering, Gaziantep University, Gaziantep, Turkey
hakanhyt@hotmail.com, yumrutas@gantep.edu.tr, sait@gantep.edu.tr

(Geliş Tarihi: 08.04.2017, Kabul Tarihi: 30.11.2017)

Abstract: This study presents the experimental investigation on performance testing of a parabolic trough solar collector (PTSC) array consisting of three modules connected in series. A new test setup has been proposed to test the thermal performance of this PTSC array in compliance with ASHRAE 93-1986 standard. The experimental tests have been carried out and monitored in a number of days under cloudless sky conditions in Gaziantep. In the performance analyses, the effects of beam radiation, collector inlet temperature, ambient conditions, and the variation in mass flow rate of the working fluid were investigated. The steady-state and dynamic tests of the PTSC array were performed. The efficiency tests were conducted with thermal oil for the temperature range from 50 °C to 200 °C, and mass flow rate of 0.1 kg/s to 0.5 kg/s under steady conditions. Additionally, the experimental results were compared with the results of the theoretical study made previously and gave good coherency.

Keywords: Solar energy, Parabolic trough collector, Optical analysis, Performance testing.

KÜÇÜK-ÖLÇEKLİ BİR PROSES ISI UYGULAMASINA İLİŞKİN PARABOLİK OLUK KOLEKTÖR AĞININ PERFORMANS TESTİ

Özet: Bu çalışma, seri bağlanmış üç modülden oluşan bir parabolik oluk güneş kolektörü (POGK) ağının performans testinin deneysel olarak incelenmesini sunmaktadır. Bu POGK ağının ısıl performansının ASHRAE 93-1986 standartına uygun olarak test edilmesi için yeni bir test düzeneği önerilmiştir. Deneysel testler, Gaziantep'te bulutsuz gökyüzü koşulları altında uygulanmış ve birkaç gün boyunca izlenmiştir. Performans analizlerinde, direk ışınım, kolektör giriş sıcaklığı, ortam koşulları ve çalışma aksıyanının kütlesel akış debisinin etkileri araştırılmıştır. POGK ağının daimi-durum ve dinamik testleri gerçekleştirilmiştir. Verimlilik testleri, termal yağ kullanılarak daimi koşullar altında 50 °C ile 200 °C sıcaklık aralığı ve 0,1 kg/s ile 0,5 kg/s kütlesel debi aralığı için gerçekleştirilmiştir. Ayrıca, deney sonuçları daha önce yapılan teorik çalışma sonuçlarıyla karşılaştırılmış ve iyi tutarlılık göstermiştir.

Anahtar kelimeler: Güneş enerjisi, Parabolik oluk kolektör, Optik analiz, Performans testi.

NOMENCLATURE

A_a	Aperture area [m^2]
C	Concentration ratio
c_p	Specific heat capacity [$\text{J/kg}^\circ\text{C}$]
F_R	Heat removal factor
I	Total radiation [W/m^2]
I_b	Beam radiation [W/m^2]
I_d	Diffuse radiation [W/m^2]
\dot{m}	Mass flow rate [kg/s]
\dot{Q}_u	Useful energy gain [W]
Re	Reynolds number [= VD/v]
Re_c	Critical Reynolds number
T_a	Ambient temperature [$^\circ\text{C}$]
T_{ex}	Exit temperature [$^\circ\text{C}$]
T_{in}	Inlet temperature [$^\circ\text{C}$]
U_L	Overall loss coefficient [$\text{W/m}^2\text{°C}$]

Greek symbols

η_o	Optical efficiency
η_{PTSC}	Thermal efficiency
θ	Incidence angle [$^\circ$]

INTRODUCTION

Parabolic trough solar collector (PTSC) technology was first drawn commercially in the middle of 70's and managed to enter the market in the 80's (Fernandez-Garcia et al., 2010). Some companies manufactured and marketed a number of PTSCs which were initially developed for industrial process heat (IPH) applications. The technology has experienced a wide range of IPH applications with respect to other non-concentrating collectors in recent years because the PTSC has distinguished advantages such as high efficiency at

relatively higher temperatures (Yilmaz and Söylemez, 2016). Consequently, the PTSC is considered to be one of the most promising and mature system used in a variety of commercial and industrial applications (Mwesigye et al., 2018). On the other hand, small-scale process heat applications using PTSC have been established by many researchers, project groups and institutions over the last decade. All these efforts have leaded us to develop more efficient solar systems eliminating technical restrictions while offering alternative solutions to conventional energy systems. Additionally, the applications being made are significant to analyze system performance from the view of technical and economic feasibility. Many criteria may restrict the design stage of a thermal system so that some preliminary studies should be considered. In process heat applications, energy demand for the process depends on process type and load profile that can be supplied unsteadily and intermittently when it is assisted with solar energy. The drawbacks of using solar energy in IPH expose these types of restrictions due to its nature. Hence a solar collector to be used in a thermal system should be necessarily tested under typical operating conditions to determine the performance that is effective on energy transfer. Otherwise, a mathematical model should be made to simulate the collector under certain working conditions. Modeling the PTSC can be convenient to analyze it under different scenarios simply changing the system properties and working conditions. It provides an easy method under defined conditions which are not easily simulated. However, it may not always be a direct and accurate way due to sacrificing from the actual system behavior. Therefore, experimental or applied test results are more advantageous for field studies. When the studies conducted on performance testing in the literature have been evaluated, it is seen many studies being performed experimentally.

ANSI/ASHRAE 93 standard (ANSI/ASHRAE, 1986) maintains a fundamental methodology to determine thermal performance of tracking concentrating solar collectors under steady state conditions. This standard can be used to test the collectors outdoors in accordance with their thermal efficiency with changes in the angle of incidence between the sun's direct radiations in a specific location. Most of the performance testing has been conducted under ANSI/ASHRAE standards (Dudley et al., 1995; Kalogirou et al., 1995; Kalogirou, 1996; Brooks et al., 2006; Arasu and Sornakumar, 2007; Rosado and Escalante, 2007; Venegas-Reyes et al., 2012; Gama et al., 2013; Jaramillo et al., 2013; Coccia et al., 2015) or with different testing techniques (Xu et al., 2013; Krüger et al., 2008; Qu et al., 2010; Sagade et al., 2013). Not only performance testing under steady condition but also dynamic testing of PTSC was presented in the literature (Eskin, 1999; Fischer et al., 2006; Xu et al., 2014). However, standard testing method for performance analysis under dynamic or transient is not available. Even if collector performance testing is performed in quasi-steady state, collector systems operate under dynamic conditions.

In this study, the outdoor test results of a PTSC array with a series of three modules have been presented for steady and dynamic cases under different operating conditions. A new test setup has been proposed to test the thermal performance of this PTSC array for this purpose. The steady tests of the collector array have been performed for varying solar radiation, inlet temperature and mass flow rate. On the other hand, the dynamic tests have been applied under normal operating conditions of the collector array. Solar energy calculations for determining the optical efficiency and the useful heat gain by the HTF have been conducted for obtaining the thermal performance of the PTSC array. The measurements of ambient air were considered during the tests to be able to experience the effects of outdoor conditions.

SYSTEM DESCRIPTION

Experimental Setup

The experimental setup is basically composed of a PTSC array, a coiled heat exchanger (CHE), a brazed plate heat exchanger (BPHE), a temperature controlled electric heater (TCEH), a thermal expansion tank (TET), and a gear pump (GP). The PTSC array is composed of three collectors connected in series installed on a building roof (12 m height from the ground) in Gaziantep University (latitude 37°02'N and longitude 37°19'E) shown in Figure 1. The orientation of the PTSC array is designated as the north-south axis tracking. The tracking system is driven by a frequency-controlled double worm gear motor which is manipulated by the cooperation of a central control unit. The tracking motion is controlled by both fine positioning sun-seeking detector and external GPS (Global Positioning System). The working fluid used in the loop was selected Renolin Therm 320 as HTF. The HTF is circulated in the loops by means of frequency-controlled GP which is used to adjust the flow rate at desired value.



Figure 1. Testing setup and collector geometry.

Measurement Instruments

The temperature measurements in the experimental setup were performed by the resistance temperature detectors (Pt100, Class A) connected with two leads. The temperature dependent uncertainty of the detectors are designated by the relation of $\pm(0.15 + 0.002T)$ °C and calibrated according to the standard of IEC751:1983 (BS EN 60751:1996) by the manufacturer (Internet, 2017a).

The flowmeter was selected as Coriolis type having an accuracy of $\pm 0.1\%$ with a repeatability of less than 0.05% (Internet, 2017b) to measure the mass flow rate of the HTF circulating within the loop. Wind speed was measured by a cup anemometer which has accuracy of 0.1 m/s for the range of 5 m/s to 25 m/s (Internet, 2017c). The irradiance sensor was used to measure the global radiation by a high sensitive pyranometer with an expected uncertainty of less than 2% as daily total (Internet, 2017d). The diffuse radiation measuring was executed with a shading ball obstructing the direct beam falling onto the pyranometer. Thus, the direct beam radiation was accurately determined using the relation (Duffie and Beckman, 2005):

$$I = I_d + I_b \cos \theta_z \quad (1)$$

where θ_z is the zenith angle of the sun defined as the angle between the line of beam radiation and the normal of the horizontal surface.

During the experimental tests, data on temperature, flow, and solar radiation were gathered by the DAQ (data acquisition) devices for further analyses. For this task, 24-bit USB-2416 and USB-TEMP measurement computing DAQ devices (Internet, 2017e) were selected in order to obtain highly-accurate voltage and temperature measurements, respectively. DAQ devices are easily connected to the computer and managed by an interface software program (TracerDAQ Pro) to process data by virtual graphing and data logging.

Hydraulic Circuit

The hydraulic circuit of the test setup is represented in Figure 2. The operation task is performed as follows. The circuit operation is started with switching on the GP, and thus the HTF is circulated within the loop. The solar tracking mechanism of the PTSC array is initiated to pursue the sun. The mass flow rate is controlled by an inverter, and the flow rate is monitored on the screen of the flowmeter and computer. In the solar field, a CHE is used to control the inlet temperature by cooling the HTF with water or air at high temperatures i.e., in the vicinity of $200 \text{ }^{\circ}\text{C}$. When the temperature fluctuations become higher, the bypass vanes are opened, and the HTF is directed to the BPHE. This is made for the precise temperature control. The loop connected to the solar field via the BPHE supplies thermal power to the HTF circulated within the field when necessary. The TCEH is controlled by a PID (Proportional Integral Derivative) controller. When the operating temperature of the loop falls below the set temperature value, the TCEH is activated to increase the return-temperature of the HTF to the set operation temperature.

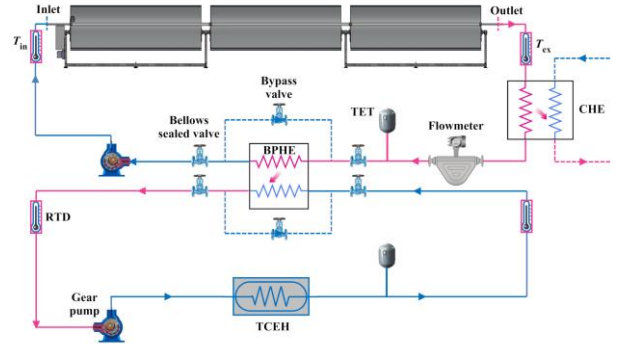


Figure 2. Hydraulic circuit.

Error Analysis

The uncertainty in experimental measurements describes the factors that are to be taken into consideration such as instrument accuracy etc. A more precise method of estimating uncertainty in experimental result has been presented by (Kline and McClintock, 1953)

The efficiency of the PTSC array is calculated from

$$\eta_{PTC} = \frac{\dot{m}c_p(T_{ex} - T_{in})}{A_a I_b \cos \theta} \quad (2)$$

Uncertainty on efficiency measurements is given by the expression,

$$w_R = \left[\left(\frac{\partial R}{\partial x_1} w_1 \right)^2 + \left(\frac{\partial R}{\partial x_2} w_2 \right)^2 + \dots + \left(\frac{\partial R}{\partial x_n} w_n \right)^2 \right]^{1/2} \quad (3)$$

where w_R is the standard uncertainty in the result and $w_1, w_2, \dots, w_{x_1}, \dots, w_n$ are the standard uncertainties of the independent variables.

$$w_\eta = \left[\left(\frac{c_p(T_{ex} - T_{in})}{A_a I_b \cos \theta} w_{\dot{m}} \right)^2 + \left(\frac{\dot{m}c_p}{A_a I_b \cos \theta} w_{A_a} \right)^2 + \left(-\frac{\dot{m}c_p(T_{ex} - T_{in})}{A_a^2 I_b \cos \theta} w_{I_b} \right)^2 \right]^{1/2} \quad (4)$$

The parameters and their measuring accuracy are given in Table 1 to calculate the uncertainty for η_{PTC} .

Table 1. Experimental error in measurements.

Measured variable	Unit	Accuracy
\dot{m}	kg/s	$\pm 0.1\%$
T	$^{\circ}\text{C}$	$\pm 0.15 + 0.002T$
A_a	m^2	$\pm 0.58\%$
I	W/m^2	$\pm 2.0\%$
η_{PTC}	—	$< \pm 6.69\%$

The errors generated from the temperature measuring devices change with temperature, besides the USB-TEMP

DAQ device contribute additional error except the error of the sensor itself. Typically, the error is ± 0.12 °C for sensor temperature (between 0 °C and 200 °C).

METHODOLOGY

In this section, the test results obtained from the experimental studies were presented in detail. The aim of the tests is to acquire the results for the PTSC characteristics and to validate it with the mathematical model developed previously (Yilmaz and Söylemez, 2014). Additionally, performance parameters of the PTSC system were analyzed under different operating conditions. Model validation for the PTSC array was performed by comparing with the experimental results. Moreover, efficiency tests were performed with temperature and mass flow rate ranging from 50 °C to 200 °C, and 0.1 kg/s to 0.5 kg/s, respectively.

Optical Performance

Optical efficiency is defined as the ratio of the beam radiation absorbed by the absorber to the energy collected by the aperture area. The optical efficiency of the collector, η_o can be defined as (Yilmaz et al., 2014)

$$\eta_o = \rho\tau\alpha\gamma(1 - \kappa\tan\theta)\cos\theta \quad (5)$$

where ρ is the reflectance of the mirror, τ is the transmittance of the glass cover, α is the absorption of the receiver, γ is the intercept factor, κ is the geometric factor, and θ is the angle of incidence.

The optical parameters of the PTSC and their typical value are given in Table 2. Each parameter was estimated or taken from the manufacturer catalogue. The optical efficiency varies as a function of incidence angle. The manufacturing company proposes the optical efficiency of Smirro300 as 0.72 when the angle of incidence is equal to zero. As the optical properties of each collector component are evaluated individually, the values shown in Table 2 are obtained. The intercept factor, γ is estimated using the data proposed by the manufacturer (see Table 2) and Eq. (5).

Table 2. Optical parameters of the PTSC.

Parameter	Value	Parameter	Value
ρ	0.895	γ	0.980
τ	0.912	κ	–
α	0.950	ζ	0.947
$\eta_o = 0.72$			

Figure 3 demonstrates the variation in optical efficiency for the selected days. For calculating the incidence angle, the procedure given in (Yilmaz et al., 2014) was followed. The optical efficiency was calculated using the procedure given in (Yilmaz and Söylemez, 2014). It is clear that increase in the incidence angle decreases the optical efficiency which is strongly dependent on the

incidence. The main reason is that higher the incidence angle lowers the beam radiation falling onto the aperture and reduces the effective aperture area due to geometric factor including end-effect. The tracking angle (the angle between the sun's rays and the normal of the aperture area) reduces in summer season relative to winter for north-south axis tracking. And thus the optical efficiency is started to get flatter in solar noon in this season.

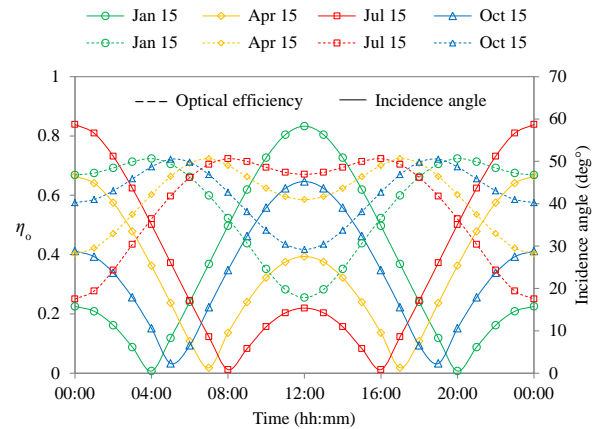


Figure 3. Variation of optical efficiency as a function of incidence angle.

Thermal Analysis

The PTSC array was tested and monitored though the tests conducted from the 15th to 21th of August 2013. The thermal performance of the PTSC array was performed in a test setup where similar test conditions were applied in accord with the ASHRAE 93-1986 (RA 91) standard (ANSI/ASHRAE, 1986). Useful heat gained by the solar field and the thermal efficiency of the PTSC array were investigated by operating the test setup at different working conditions. The performance of the PTSC was evaluated by using the parameters; beam radiation, and inlet and outlet temperatures of the HTF through the absorber tube for a given mass flow rate. In calculations, the thermophysical properties given in Table 3 were used for the HTF.

Table 3. Technical properties of the HTF^a.

Temp. °C	Density kg/m ³	Specific heat J/kg·°C	Thermal conductivity W/m·°C	Kinematic viscosity m ² /s × 10 ⁻⁶
0	879	1864	0.134	368.39
50	848	2078	0.131	22.144
100	816	2293	0.127	5.535
150	783	2507	0.124	2.463
200	750	2721	0.120	1.416

^a Supplier: Opet Fuchs Mineral Oil Industry and Trade Inc., Izmir, Turkey.

Time constant

The collector time constant is the time required for the fluid leaving the PTSC array to attain 63.2% of its ultimate steady-state value after a step change in irradiance. This parameter determines the collector's time response for the evaluation of transient behavior of the collector and the subsequent selection of correct time interval to maintain quasi steady-state efficiency tests.

The time constant of PTSCs was obtained by

$$\frac{T_{ex} - T_{ex,t}}{T_{ex} - T_{in}} = \frac{1}{e} = 0.368 \quad (6)$$

where T_{in} is the temperature at the collector inlet to be set approximately equal to the ambient air temperature, T_{ex} is the final temperature at the collector outlet, and $T_{ex,t}$ is the temperature at the collector outlet to maintain the steady-state conditions again for a time period of t .

The time constant for heating determines the time required for the collector outlet temperature to rise by 63.2% of the temperature difference $T_{ex} - T_{in}$. The time constant for cooling, in this case, is the time taken for the collector outlet temperature to drop by 63.2% of the temperature difference $T_{ex} - T_{in}$. The procedure for performing this test is as follows. The HTF is circulated through the collector array at the same flow rate to be used during collector thermal efficiency tests. The PTSC array is defocused, and temperature of the HTF at the collector inlet is set closely equal to the ambient air temperature. As the steady-state conditions are reached, the collector array is focused and measurements continue until steady-state conditions are attained again.

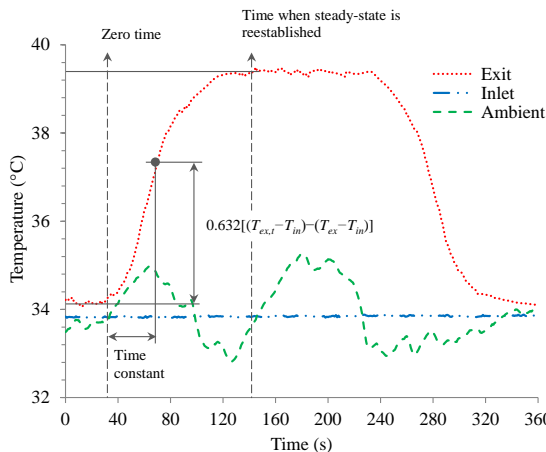


Figure 4. Time constant for heating of the receiver tube.

Figure 4 shows the heating operation to determine the time constant of the PTSC receiver. The mass flow rate for HTF was carried out 0.3 kg/s, and the beam radiation was measured as 845 W/m² during the test. The time constant for heating and cooling processes were obtained to be 33.7 s and 53.1 s, respectively. As it is known, the time constant varies with changing in the flow rate.

Increase in flow rate decreases the time and thus the time constant for the PTSC to reach the steady conditions. Therefore, the time period which is needed to carry out the performance tests is either at least the time constant or more than this time period. The duration of time for the tests was taken into account as 2 minutes to obtain feasible results.

Useful heat gain

The net energy transferred to the HTF by the solar field is related by the useful heat gain which leads the temperature change for the HTF flowing through the receiver tube of the PTSC array. The energy gained by the HTF can be calculated by using Eq. (7).

$$\dot{Q}_u = \dot{m}_{HTF} c_{p,HTF} (T_{ex} - T_{in}) \quad (7)$$

The useful heat gain is important to determine the outlet temperature and the net energy transfer to the working fluid. This means that the thermal efficiency of the PTSC depends on the useful heat gained by the HTF.

Thermal efficiency

The thermal efficiency of the PTSC array is defined as the ratio of the useful heat transferred the HTF to the beam radiation incident on the aperture area of the array (Yilmaz and Söylemez, 2014).

$$\eta_{PTSC} = \frac{\dot{Q}_u}{A_a \times I_b} = F_R \left[\eta_o - \frac{U_L}{C} \left(\frac{T_{in} - T_a}{I_b} \right) \right] \quad (8)$$

The first expression in the equation is derived directly from the experimentally measurable quantities, and the second expression can be obtained by applying the energy balance. η_o is the optical efficiency defined in Eq. (5). The heat removal factor F_R and the overall loss coefficient U_L depend on heat losses and are independent of the angle of incidence.

RESULTS AND DISCUSSION

The general test procedure was arranged to operate the PTSC system under nearly steady conditions. This is essential to measure the test data for the determination of the useful heat gain given in Eq. (7) and T_{in} , T_a and I_b parameters which are needed for the analysis of Eq. (8). Outdoor tests were performed in the midday hours on clear days when the beam radiation is high and the incidence conditions almost the same. However, $\tau\alpha$ deviates from the normal-incidence value for the test conditions being involved. Thus, the optical efficiency somewhat falls according to the increase in the incidence angle.

In case U_L , F_R , and $(\tau\alpha)_n$ were all constant, the plots of η_{PTC} versus $(T_{in} - T_a)/I_b$ would be straight lines with intercept $F_R(\tau\alpha)_n$ and slope $-F_R U_L$ (Duffie and Beckman, 2005). However, they are not since U_L is a function of

temperature and wind speed. F_R is a weak function of temperature. Also, some variations on beam radiation and incidence angle will not maintain a steady line. Thus, scatter in the data are to be expected, because of temperature dependence, wind effects, and angle-of-incidence variations. In spite of these difficulties, long-time performance estimates of many solar heating systems, collectors can be characterized by the intercept and slope i.e., by $F_R(\tau\alpha)_n$ and $F_R U_L$. But the linear relation instead of second degree polynomial relation is generally acceptable in the case of considering solar concentrators operating at low temperature.

Figure 5 shows the variation in the experimental thermal efficiency of the PTSC array depending on $(T_{in} - T_a)/I_b$. It is also indicated the predictions of our previous theoretical model (Yılmaz and Söylemez, 2014) on this figure. Tests were conducted in the clear sky days and the incident conditions of almost solar noon (at 12:00 solar time) in order to do the tests almost under the same incidence angle values. The incidence angle calculated during the tests ranged from 20° to 24.5° . The mass flow rate for the HTF was chosen as 0.3 kg/s , and the inlet temperature of the HTF ranged from 85°C to 200°C . The efficiency tests were performed at higher temperatures due to the fact that at lower temperatures, the flow inside the receiver is in laminar regime. The HTF enters the turbulent regime at higher temperatures, in turn; this condition increases the thermal efficiency. In case the fluid is exchanged with water, the fluid regime will be in turbulent region even at lower temperatures. The efficiency tests made in the literature involve water as a HTF. In fact, to analyze the thermal performance of a PTSC, low temperature tests are carried out as in the ASHRAE standards. Thus, the maximum efficiency of the PTSC is investigated.

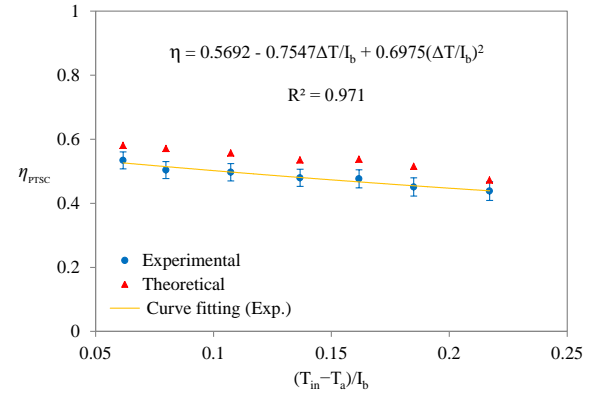


Figure 5. Experimental results and fit of the thermal efficiency of Smirro300.

The experimental data were fitted to a second-degree polynomial function to represent the variation in the thermal efficiency as shown in Figure 5. The coefficient of determination R^2 shows how good this function fit the experimental data, and the deviation between the data and the correlation. It is deduced that the thermal efficiency of the PTSC array is higher at lower inlet HTF temperatures since the heat loss from the receiver is lower with respect to high ones. Depending on the incident conditions, the PTSC array can give maximum 57% efficiency which means that that portion of solar energy can be converted into the useful heat gain.

In case of comparing this efficiency curve with the efficiency expressions (see Table 4) available in the literature, although PTSCs tests in literature are applied for the conditions of single module collector, direct incident conditions (the incident angle $\approx 0^\circ$) and water used as a working fluid, Smirro300 PTSC array gave favorable efficiency values relative to the others. In order to compare Smirro300 with other PTSCs, the model study is succeeded for different operating conditions as seen Table 5.

Table 4. Comparison of different PTSC parameters^{b,c}.

Reference	C	φ_r	η_o	γ	τ	α	ρ	η_{PTC}
5	21.2	90°	0.648	0.98	n/a	n/a	n/a	$0.642-0.441T^*$
6	21.2	90°	0.647	0.94	0.90	0.90	0.85	$0.638-0.387T^*$
7	16.7	82.2°	0.553	0.823	0.92	0.88	0.83	$0.538-1.06T^*$
7	16.7	82.2°	0.601	0.823	–	0.88	0.83	$0.552-2.01T^*$
8	19.89	90°	0.694	0.879	0.90	0.90	0.97	$0.69-0.39T^*$
9	34.84	65.6°	n/a	n/a	0.95	0.95	0.59	$0.054-0.189T^*$
10	14.87	45°	0.60	0.665	–	0.95	0.95	$0.561-2.047T^*$
11	14.9	45°	0.48	0.58	–	0.90	0.92	$0.351-2.117T^*$
11	13.3	90°	0.70	0.84	–	0.90	0.92	$0.613-2.302T^*$
12	9.25	90°	0.668	0.829	0.93	0.95	0.94	$0.658-0.683T^*$

^b $T^* = (T_{in} - T_a)/I_b$.

^c (–) indicates that the receiver considered is unshielded.

Table 5. Thermal performance of the PTSC.

Case	Angle	Fluid	η_{PTC} theoretical ^d
Single	$\theta = 0^\circ$	Renolin	$0.659 + 0.176\Delta T/I_b - 2.979(\Delta T/I_b)^2$
Single	$\theta = 0^\circ$	Water	$0.719 - 0.457\Delta T/I_b$
Single	$\theta \approx 22^\circ$	Renolin	$0.590 + 0.088\Delta T/I_b - 2.383(\Delta T/I_b)^2$
Array	$\theta = 0^\circ$	Renolin	$0.652 + 0.176\Delta T/I_b - 2.251(\Delta T/I_b)^2$
Array	$\theta = 0^\circ$	Water	$0.718 - 0.520\Delta T/I_b$
Array	$\theta \approx 22^\circ$	Renolin	$0.582 + 0.078\Delta T/I_b - 2.573(\Delta T/I_b)^2$
η_{PTC} experimental ^d			
Array	$\theta \approx 22^\circ$	Renolin	$0.569 - 0.755\Delta T/I_b + 0.697(\Delta T/I_b)^2$

^d Tested at 0.3 kg/s.

Table 5 demonstrates the results obtained from the model study for different cases. As the incident angle is minimized, the efficiency of the PTSC array increases since the cosine losses reduce. If the PTSC array is

replaced with a single module, the efficiency will increase but not much. This is expected since this case affects the F_R value which decreases when the receiver length gets longer. As the working fluid type is changed as water, and the model yields much higher efficiencies depending on the parameter of $(T_{in} - T_a)/I_b$.

The dynamic behaviors of the PTSC are illustrated in Figure 6, 7 and 8. The HTF was heated from 50 °C to 220 °C by solar radiation under ambient conditions. The flow rate was adjusted by the GP with a constant frequency-control while heating the solar field. The flow rate was changed as a function of outlet temperature of the PTSC; $\dot{m} = 1141 - 1.010T_{ex}$, $\dot{m} = 1142 - 0.9829T_{ex}$ and $\dot{m} = 1210 - 1.065T_{ex}$ for the days of 15th, 17th and 21th August, respectively. Here the unit of \dot{m} is in kg per hour. The variations in the inlet and the exit temperatures and the thermal efficiency are shown in detail.

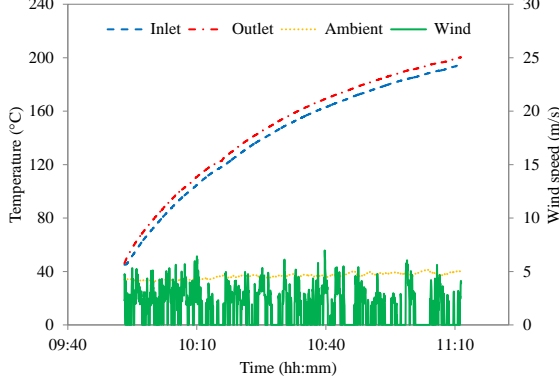


Figure 6. Dynamic operation profile on August 15.

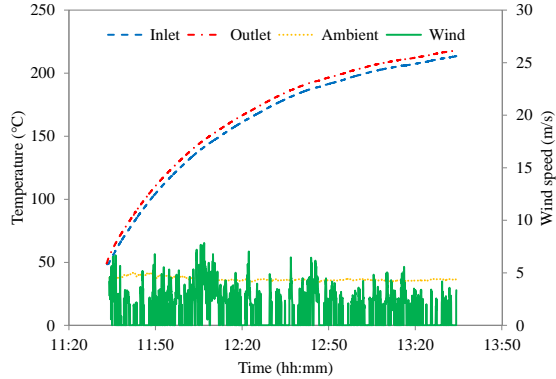


Figure 7. Dynamic operation profile on August 17.

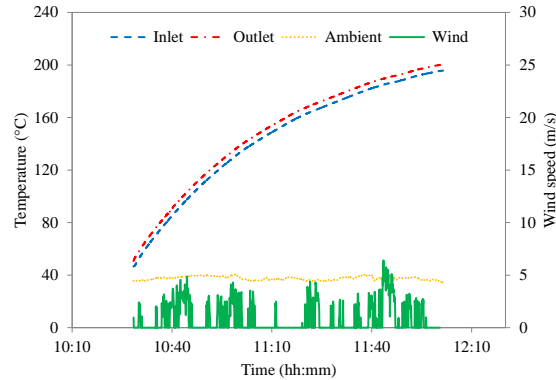
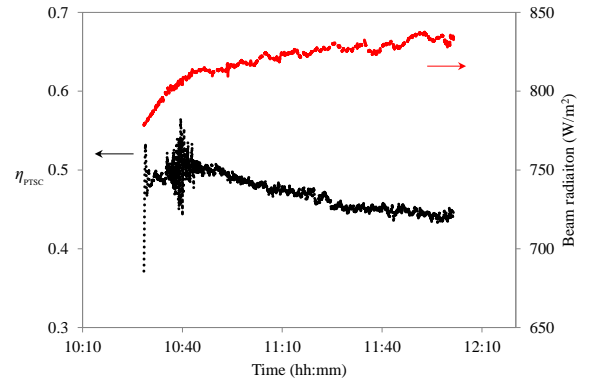
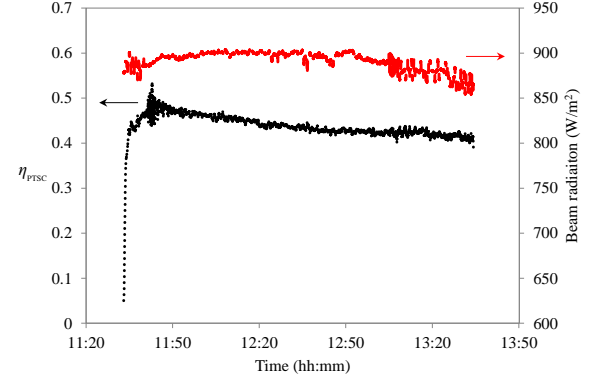
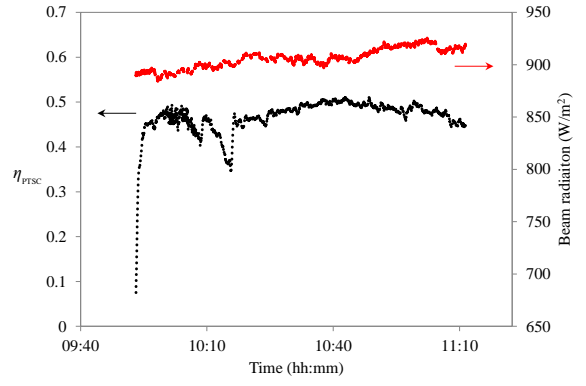


Figure 8. Dynamic operation profile on August 21.



As the HTF temperature increases, the heat losses from the receiver and system components increase. Thus, the temperature profile tends to be upward sloping curve. In other words, the thermal efficiency of the PTSC begins to fall with increasing of the operating temperature. The thermal efficiency strongly depends on incident beam radiation, optical efficiency of the PTSC, and operating conditions. Operating conditions such as temperature and flow regime affect predominantly the thermal efficiency (Yilmaz and Söylemez, 2014; Yilmaz et al., 2015). Between 80 °C and 100 °C, the thermal efficiency fluctuates due to transition regime. The flow inside the pipe is stated by forced circulation due to pumping of the HTF. The single control parameter is the Reynolds number (Re), which determines the dynamical state of the system. Hence when $Re < Re_c$, all initial conditions are attracted to the laminar state, which is the global attractor for the system. When $Re \gg Re_c$, nearly all initial conditions give rise to turbulence so that the laminar state becomes a local attractor. In practice, $Re_c \lesssim 1800$ so that all disturbances will decay as the time extends to the very long periods for small values of Re (Mullin, 2011). Turbulence appears abruptly above a well-defined finite-amplitude threshold for $Re \gtrsim 3000$, but the disordered motions come out in localized regions called *puffs* in the range of $1760 \lesssim Re \gtrsim 3000$. In thermal oils, Re increases relatively at higher mass flow rates and temperatures, depending on the thermophysical properties of the fluid. Increasing in the mass flow rate causes to develop turbulent currents within the absorber pipe so that the thermal efficiency of the PTSC rises. This is related to the HTF which absorbs more energy from the inner surface of the pipe. The higher the mass flow rate, the higher the fluid motion or Re , as a result the convection heat transfer coefficient within the absorber tube is increased. This leads the inside temperature of the absorber to fall down thus the useful heat gain transferred to the fluid increases due to lowering thermal loss. Raising the operating temperature of HTF increases the Re and consequently the convection currents within the absorber.

Figure 9 points out the variation in mass flow rate and its effect on the thermal efficiency. The thermal performances are analyzed for the inlet temperatures of 50 °C, 100 °C, 150 °C and 200 °C, respectively. At these temperatures, the effect of mass flow rate of the HTF was performed from the range of 0.1 kg/s to 0.5 kg/s. For each try, the receiver of the PTSC array was directed toward the sun by the tracking mechanism. The inlet temperature was initially provided as 50 °C at which the mass flow rates from 0.1 kg/s to 0.5 kg/s were experienced, and then 100 °C, 150 °C and 200 °C temperatures were dealt with for the same flow rates.

It is expected that the increase in the mass flow rate enhances the thermal efficiency. At lower flow rates and temperatures, the regime of the flow is in laminar or transition region which degrades the convection heat transfer coefficient within the absorber pipe hence the thermal efficiency of the collector drops as seen in Figure 9. At 50 °C inlet temperature, increasing the mass flow rate from 0.1 to 0.5 increases the Re from 212 to 1058.

Thus, the flow regime remains in laminar zone which is related to the viscosity of the HTF. The disordered motions come out about 80 °C which corresponds to the Re of 1700. When the inlet temperature increases to 100 °C, the viscosity of the HTF lowers about one-fourth relative to the viscosity at 50 °C, and the Re rises to 4405 while the mass flow rate is 0.5 kg/s. Further increasing the temperature declines the viscosity much more. At 200 °C, as the mass flow rate reaches 0.5 kg/s, the Re ascends to 18733 that is quite higher than the generally accepted value ($Re > 10000$ under most practical conditions (Gnielinski, 1976)) for fully turbulent. As it is shown in Figure 9, increasing the temperature increases the thermal efficiency but can be lowered due to wind effect. The effect of wind is considerable on the thermal efficiency over those higher speeds when the PTSC is operated at relatively high temperatures (Yilmaz and Söylemez, 2014). As it is seen, the wind speed is more effective at 200 °C although it is lower relative to 100 °C.

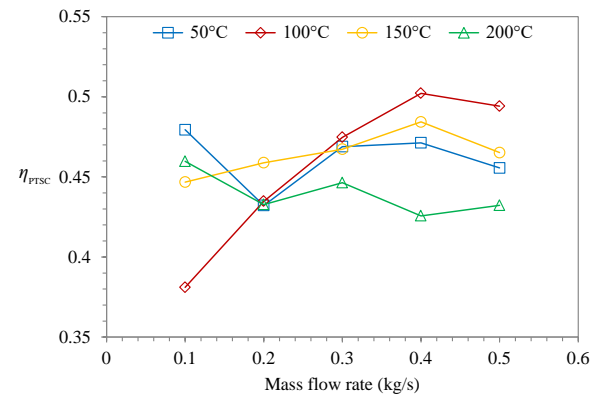


Figure 9. Effect of mass flow rate on the thermal efficiency.

The thermal efficiency depends upon both optical and thermal properties of the PTSC. The optical efficiency depends also on many parameters as mentioned previously. They are mainly function of material used, manufacturing stage, assembling, operation and geometric conditions. In addition, unaccounted parameters such as dust, dirty are effective on the optical elements. Smirro300 PTSC can reach a peak optical efficiency of 72% only when the direct incident and proper assembly conditions are applied. In the experimental setup, the PTSC array was oriented to N-S direction which was adjusted by aligning the focus line of the receiver towards the direction. Any deviation from this line will degrade the intercept factor, and consequently the optical efficiency. Since these errors are non-random in nature and can reduce the collector performance. For a single collector, this error may be disregarded but in array configuration, in case of driving the collectors only by a single tracking mechanism, this should be taken into consideration. On the other hand, the concentricity between the cover and absorber is essential during assembly. If it is not maintained properly it will affect the optical efficiency in negative way. During the tracking operation, the end-effect also influences the optical efficiency, and its effect is under predicted in theoretical calculations. Since the receiver is single-

piece, and the gap between the collectors increase the optical loss for this reason.

CONCLUSIONS

Parabolic trough solar collector is a proven technology for electricity generation but its usage in IPH applications have not been matured completely, yet. In this study, the sample performance tests of Smirro300 collector were performed to characterize it under the climate conditions of Gaziantep. An experimental setup was installed for this task, and the necessary analyses were carried out for the future studies to be made on a small-scale IPH. All these efforts will play an important role in the related system design and the methodology to be followed experimentally. Furthermore, a new test setup has been proposed to test the thermal performance of the PTSC in compliance with ASHRAE 93-1986 standard. On the other hand, the experimental results obtained from performance testing of the PTSC array were compared to the theoretical study (Yilmaz and Söylemez, 2014) and showed good coherency with the proposed mathematical model. The performance tests showed that the obtained characteristic curve of the tested collector is considerably favorable for IPH applications requiring thermal energy need lower than 200 °C (Yilmaz et al., 2014b).

ACKNOWLEDGEMENT

This study was funded by the scientific research project unit of GAÜN under the contract of MF.11.13. Any opinions, findings, and conclusions or recommendations expressed in this study are those of the authors and do not necessarily reflect the views of the project unit.

REFERENCES

- ANSI/ASHRAE 93-1986 (RA91), 1986, Methods of Testing to Determine the Thermal Performance of Solar Collectors.
- Arasu A. V. and Sornakumar T., 2007, Design, manufacture and testing of fiberglass reinforced parabola trough for parabolic trough solar collectors, *Sol. Energy*, 81, 1273–1279.
- Brooks M. J., Mills I. and Harms T. M., 2006, Performance of a parabolic trough solar collector. *J. Energy South Afr.*, 17(3), 71–80.
- Coccia G., Nicola G. D. and Sotte M., 2015, Design, manufacture, and test of a prototype for a parabolic trough collector for industrial process heat, *Renew. Energ.*, 74, 727–736.
- Dudley V. E., Evans L. R. and Matthews C. V., 1995, *Test Results – Industrial Solar Technology Parabolic Trough Solar Collector*. Sandia National Laboratories, SAND94-1117.
- Duffie J. A. and Beckman W. A., 2005, *Solar engineering of thermal processes* (Third Ed.), John Wiley & Sons, New York.
- Eskin N., 1999, Transient performance analysis of cylindrical parabolic concentrating collectors and comparison with experimental, *Energ. Convers. Manage.*, 40, 175–191.
- Fernandez-Garcia A., Zarza E., Valenzuela L. and Perez M., 2010, Parabolic-trough solar collectors and their applications, *Renew. Sust. Energ. Rev.*, 14, 1695–1721.
- Fischer S., Lüpfert E. and Müller-Steinhagen H., 2006, Efficiency testing of parabolic trough collectors using the quasi-dynamic test procedure according to the European standard EN 12975, *SolarPACES 13th Symposium on Concentrating Solar power and Chemical Energy Technologies*, Seville, Spain.
- Gama A., Larbes C., Malek A., Yettou F. and Adouane B., 2013, Design and realization of a novel sun tracking system with absorber displacement for parabolic trough collectors, *J. Renew. Sustain. Ener.*, 5, 033108–1/18.
- Gnielinski V., 1976, New equations for heat and mass transfer in turbulent pipe and channel flow, *Int. Chem. Eng.*, 16, 359–68.
- Internet, 2017a, *Technical datasheet of Pt100*, <http://www.ordel.com.tr>.
- Internet, 2017b, *Optimass 6000 technical datasheet*, <http://www.krohne.com>.
- Internet, 2017c, *Type 40 maximum anemometer*, <http://www.renewablenrgsystems.com>.
- Internet, 2017d, *Technical datasheet of CMP11*, <http://www.kippzonen.com>.
- Internet, 2017e, *USB-2416 and USB-TEMP User's Guide*, <http://www.mccdaq.com>.
- Jaramillo O. A., Venegas-Reyes E., Aguilar J. O., Castrejón-García R. and Sosa-Montemayor F., 2013, Parabolic trough concentrators for low enthalpy processes, *Renew. Energ.*, 60, 529–539.
- Kalogirou S. A., Lloyd S., Ward J. and Eleftheriou P., 1994, Design and Performance Characteristics of a Parabolic-Trough Solar-Collector System, *Appl. Energ.*, 47, 341–354.
- Kalogirou S., 1996, Parabolic Trough Collector System for Low Temperature Steam Generation: Design and Performance Characteristics, *Appl. Energ.*, 55, 1–19.
- Kline S. J. and McClintock F. A. 1953, Describing uncertainties in single-sample experiments, *Mech. Eng.*, 75(1), 3–8.

- Krüger D., Pandian Y., Hennecke K. and Schmitz K., 2008, Parabolic trough collector testing in the frame of the REACT project, *Desalination*, 220, 612–618.
- Mullin T., 2011, Experimental studies of transition to turbulence in a pipe, *Annu. Rev. Fluid Mech.*, 43, 1–24.
- Mwesigye A., Yılmaz İ. H. and Meyer J. P., 2018, Numerical analysis of the thermal and thermodynamic performance of a parabolic trough solar collector using SWCNTs-Therminol®VP-1 nanofluid, *Renew. Energ.*, (Accepted).
- Qu M., Yin H. and Archer D. H., 2010, Experimental and Model Based Performance Analysis of a Linear Parabolic Trough Solar Collector in a High Temperature Solar Cooling and Heating System, *J. Sol. Energ.- T. ASME*, 132(2), 0210041–02100412.
- Rosado H. N. and Escalante S. M. A., 2011, Efficiency of a parabolic trough collector as a water heater system in Yucatán, Mexico, *J. Renew. Sustain. Ener.*, 3, 063108–1/6.
- Sagade A. A., Aher S. and Shinde N. N., 2013, Performance evaluation of low-cost FRP parabolic trough reflector with mild steel receiver, *Int. J. Energ. Env. Eng.*, 4(1), 5.
- Venegas-Reyes E., Jaramillo O. A., Castrejón-García R., Aguilar J. O. and Sosa-Montemayor F., 2012, Design, construction, and testing of a parabolic trough solar concentrator for hot water and low enthalpy steam generation, *J. Renew. Sustain. Ener.*, 4, 053103–1/18.
- Xu L., Wang Z., Li X., Yuan G., Sun F. and Lei D., 2013, Dynamic test model for the transient thermal performance of parabolic trough solar collectors, *Sol. Energy*, 95, 65–78.
- Xu L., Wang Z., Li X., Yuan G., Sun F., Lei D. and Li S., 2014, A comparison of three test methods for determining the thermal performance of parabolic trough solar collectors, *Sol. Energy*, 99, 11–27.
- Yılmaz İ. H., Söylemez M. S., Hayta H. and Yumrutaş R., 2014a, Model-Based Performance Analysis of a Concentrating Parabolic Trough Collector Array, *Progress in Exergy, Energy, and the Environment*, Springer, Cham.
- Yılmaz İ. H., Söylemez M. S., Hayta H. and Yumrutaş R., 2014b, A Process Heat Application Using Parabolic Trough Collector, *Springer Proceedings in Physics* (Vol. 155), Springer, Switzerland.
- Yılmaz İ. H. and Söylemez M. S., 2014, Thermo-mathematical modeling of parabolic trough collector, *Energ. Convers. Manage.*, 88, 768–784.
- Yılmaz İ. H., Hayta H., Yumrutaş R. and Söylemez M. S., 2015, Performance Testing of A Parabolic Trough Collector Array. *The 6th International Congress of Energy and Environment Engineering and Management (CIEM15)*, Paris, France.
- Yılmaz İ. H., Söylemez M. S., 2016, Transient simulation of solar assisted wheat cooking by parabolic trough collector, *J. Glob. Eng. Stud.*, 3(1), 93–106.



Ibrahim Halil YILMAZ graduated from Department of Mechanical Engineering at Gaziantep University. He received M.Sc. degree and Ph.D. degree in energy area at the same department in 2009 and 2014, respectively. He worked in several positions at Gaziantep University between 2007–2016 and at Zurich Technopark in 2009 as a visiting researcher. He is currently Assistant Professor in the Department of Automotive Engineering, Adana Science and Technology University. He is the author or co-author of more than 25 technical papers in the international journals or conferences. His main research interests lie in the area of renewable, clean and sustainable energy systems, thermal system design, analytical & numerical heat transfer/fluid flow, thermal system modeling, refrigeration systems, and energy projection scenarios of biomass & municipal solid waste.



Hakan HAYTA graduated from Department of Mechanical Engineering at Gaziantep University. He received M.Sc. degree in energy area at the same department in 2015. He lectured several courses in Vocational School of Gaziantep University between 2011–2015. He is the general manager of Lider Engineering Co. where he has managed a great number of energy related projects since 2008. His main working areas are conventional heating systems, heating, cooling & ventilating systems, heat pumps, solar energy, photovoltaic systems.



Recep YUMRUTAŞ graduated from Department of Mechanical Engineering at Middle East Technical University in 1988. He received M.Sc. degree in energy area at Gaziantep University in 1991. He got his Ph.D. degrees in 1998 from Gaziantep University and Suleyman Demirel University, respectively. He attended in Vocational School of Gaziantep University in 1998. He received Assistant Professor, Associate Professor and Professor degrees in Energy, Mechanical Engineering Department in 2000, 2009 and 2015, respectively. He is the author or co-author of about 100 technical papers in the international journals or conferences. His main research interests are heating, cooling, heat pumps, solar energy, energy storage, modeling of thermal systems, insulating materials, valorization of waste oil & tire for internal combustion engines.



Mehmet Sait SÖYLEMEZ graduated from Department of Mechanical Engineering at Middle East Technical University in 1985. He received M.Sc. degree on solar energy at Middle East Technical University in 1988. He got his Ph.D. degree on natural convection in 1992 from Gaziantep University. He became Professor at Mechanical Engineering Department in 2006. He has published more than 50 technical papers in the international journals or conferences. His main research areas are refrigeration, heat pumps, solar energy, and thermo-economic optimization.